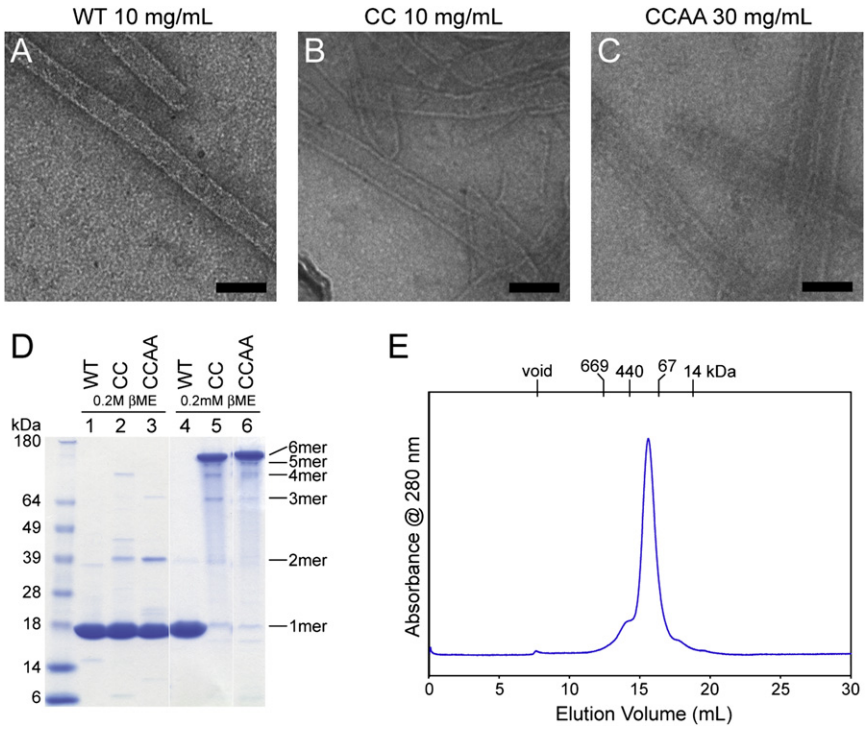

Figure 1. Stabilization of the HIV-1 CA Hexamer by Thiol Crosslinking

(A–C) Cylinders assembled in vitro from pure wild-type HIV-1 CA (A), A14C/E45C (B), and A14C/E45C/W184A/M185A (C), stained with uranyl acetate, and visualized via transmission electron microscopy. The scale bars represent 100 nm.

(D) Nonreducing SDS-PAGE analysis of in vitro assembly reactions, with wild-type CA (lanes 1 and 4), A14C/E45C (lanes 2 and 5), and A14C/E45C/W184A/M185A (lanes 3 and 6) after assembly under reducing conditions (lanes 1–3), and after crosslinking (lanes 4–6). Molecular weight markers are labeled on the left, and the positions of crosslinked CA oligomers (n = 1–6) are indicated on the right. Note that n > 6 oligomers were not observed, supporting the conclusion that disulfide bond formation is not driven by random diffusional encounters, but by specific interactions within the assembled cylinders.

(E) Size exclusion chromatographic profile of discrete hexamers of crosslinked A14C/E45C/W184A/M185A. Elution volumes of protein standards are indicated.

hexamerization. In the former case, the cryoEM-based coordinate model of the HIV-1 CA lattice (PDB code 3dik) (Ganser-Pornillos et al., 2007) was examined to identify residue pairs that appeared to be in close contact across the NTD-NTD interface. Cysteines were introduced at these positions, and the mutant CA proteins were assembled under reducing conditions into cylinders, which are known to faithfully mimic the hexagonal portion of the HIV-1 capsid (Briggs et al., 2003; Campbell and Vogt, 1995; Ehrlich et al., 1992; Ganser-Pornillos et al., 2004; Gross et al., 1997; Li et al., 2000). Our expectation was that, within the assembled cylinders, one or more of the engineered cysteine pairs would be positioned optimally to form intermolecular disulfide bonds and, upon oxidation, create a covalently linked hexamer. This approach also provided a functional check for the mutant proteins.

As shown in Figure 1, a construct with cysteine substitutions for A14 and E45 assembled into cylinders that were morphologically very similar to those formed by the wild-type protein (compare Figures 1A and 1B). Upon oxidative crosslinking, the CA subunits from these assemblies migrated almost exclusively as hexamers in nonreducing SDS-PAGE gels (Figure 1D, lane 5). Indeed, complete crosslinking was observed even in the presence of a 500-fold molar excess of reducing agent (data not shown), demonstrating that disulfide bond formation was driven by the specific noncovalent protein-protein interactions within the cylinders. Not surprisingly, the crosslinked cylinders were extraordinarily stable, and remained intact under conditions in which wild-type cylinders readily disassembled (e.g., low salt, or in the presence of the proline rotamase cyclophilin A) (data not shown). To obtain isolated hexamers for crystallization, we therefore introduced two additional mutations (W184A and M185A) at the CTD-CTD interface, to weaken the extended lattice (Gamble et al., 1997; von Schwedler et al., 2003) while leaving the hexamer-stabilizing interfaces unchanged further. This CA construct assembled less efficiently but still formed cylinders (Figure 1C). More important, it crosslinked into discrete, soluble hexamers with ~100% efficiency (Figure 1D, lane 6, and Figure 1E).

Our second approach for creating discrete hexamers was to fuse the CcmK4 protein to the C-terminal end of HIV-1 CA. CcmK4 forms stable hexameric rings in solution and has accessible termini (Kerfeld et al., 2005), making it an attractive template for driving CA hexamerization. Various linker lengths and sequences were tested, and all of the CA-CcmK4 fusion proteins that expressed solubly were also hexameric in solution, as analyzed by analytical equilibrium sedimentation (data not shown). However, different constructs eluted with different retention times by gel filtration, and we assumed that only the constructs that behaved as apparent hexamers (late eluters) were correctly folded (data not shown). The successful construct consisted of CA residues 1–226, a two-residue linker, and the full-length CcmK4 sequence followed by the remains of an affinity tag. As in the crosslinked construct, it was necessary to introduce the W184A and M185A mutations to the CTD region to prevent the hexamers from polymerizing into insoluble aggregates.

Architecture of the CA Hexamer

Four crystallographically independent models of the HIV-1 CA hexamer were derived. The first model was obtained from crystals of CcmK4-templated CA, and was determined to 7 Å resolution (Figure S1 available online; see Table 1 for crystallographic statistics). The remaining three hexamer models were determined from two different crystal forms of crosslinked CA, which diffracted to 1.9 and 2.7 Å resolution (Figures S2 and S3; Table 1).

The quaternary organization of the crosslinked and templated hexamers are identical (to the limit of their respective resolutions)